ISSN 0036-0236, Russian Journal of Inorganic Chemistry, 2016, Vol. 61, No. 5, pp. 623–629. © Pleiades Publishing, Ltd., 2016.
Original Russian Text © V.I. Pet'kov, A.S. Dmitrienko, M.V. Sukhanov, A.M. Koval'skii, E.Yu. Borovikova, 2016, published in Zhurnal Neorganicheskoi Khimii, 2016, Vol. 61, No. 5, pp. 654–660.

PHYSICAL METHODS OF INVESTIGATION

Synthesis, Phase Formation, and Thermal Expansion of Sulfate Phosphates with the $NaZr_2(PO_4)_3$ Structure

V. I. Pet'kov[a], A. S. Dmitrienko[a], M. V. Sukhanov[a], A. M. Koval'skii[b], and E. Yu. Borovikova[c]

[a] *Lobachevsky State University of Nizhny Novgorod, pr. Gagarina 23, Nizhny Novgorod, 603950 Russia*
[b] *National University of Science and Technology MISiS, Moscow, Russia*
[c] *Moscow State University, Vorob'evy gory, Moscow, 119991 Russia*
e-mail: petkov@inbox.ru

Received June 5, 2015

Abstract—The $NaFeZr(PO_4)_2SO_4$ and $Pb_{2/3}FeZr(PO_4)_{7/3}(SO_4)_{2/3}$ sulfate phosphates with the $NaZr_2(PO_4)_3$ (NZP) structure were synthesized and studied using X-ray diffraction, electron microprobe analysis, IR spectroscopy, and simultaneous differential thermal and thermogravimetric analysis. The phase formation and thermal stability of the compounds were studied by powder X-ray diffraction and DTA–TG. The $Pb_{2/3}FeZr(PO_4)_{7/3}(SO_4)_{2/3}$ structure was refined by full-profile analysis. The structure framework is composed of randomly occupied $(Fe,Zr)O_6$ octahedra and $(P,S)O_4$ tetrahedra; the Pb^{2+} ions occupy extra-framework sites. The thermal expansion of $Pb_{2/3}FeZr(PO_4)_{7/3}(SO_4)_{2/3}$ in the temperature range from −120 to 200°C was studied by temperature X-ray diffraction. In terms of the average linear coefficient of thermal expansion ($\alpha_{av} = 1.7 \times 10^{-6}{}^{\circ}C^{-1}$), this compound can be classified as having low expansion. The combination of different tetrahedral anions (a phosphorus and a smaller sulfur one) in the NZP resulted in a decrease in the framework size and cavities and enabled the preparation of low-expansion sulfate phosphate with a smaller extra-framework cation (cheap Pb) instead of larger cations (Cs, Ba, Sr) used most often in the monoanionic phosphates.

DOI: 10.1134/S0036023616050168

The good prospects of using mixed phosphates, structural analogs of the kosnarite $KZr_2(PO_4)_3$, isostructural to a large class of solid ionic conductors, NASICON and $NaZr_2(PO_4)_3$ (NZP), containing additional tetrahedral TO_4 anions (T = Mo, As, V, Si, B), originate from new or improved properties as compared with monoanionic phosphates [1–7]. The crystal chemical criteria enabling the existence of properties such as superionic conduction and ultralow thermal expansion have been elaborated to a certain extent and have some predictive power [8, 9]. For example, upon $P^{5+} \rightarrow As^{5+}$ and $P^{5+} \rightarrow Si^{4+}$ isomorphous substitutions, the unit cell volume of the $LiZr_2As_xP_{3-x}O_{12}$ and $Na_{1+x}Zr_2Si_xP_{3-x}O_{12}$ solid solutions increases in accordance with the relationship between the P^{5+} and As^{5+} or Si^{4+} ionic radii. The absence of steric hindrance for the migration of lithium and sodium ions along the migration channels and increase in the vacant sity occupancy in the crystal lattice by mobile sodium ions bring about an increase in the ionic conduction with respect to that of phosphates ($x = 0$) [8, 10].

The NZP phosphates with large Cs, Sr, and Ba cations in the structure cavities, namely $CsZr_2(PO_4)_3$, $CsHf_2(PO_4)_3$, $Sr_{0.5}Zr_2(PO_4)_3$, $K_{0.5}Sr_{0.25}Zr_2(PO_4)_3$, and $Ca_{0.38}Ba_{0.12}Zr_2(PO_4)_3$ [11–15], have nearly zero linear thermal expansion coefficients (LTECs) and expansion anisotropy values. They can serve for the fabrication of thermomechanically stable materials able to withstand repeated sharp changes in the heat load [16]. The targeted combination of different tetrahedral anions, of which one is phosphorus and the other (smaller) one is sulfur, in an NZP would decrease the framework dimensions and cavities, enable correction of the LTEC of sulfate phosphates toward lower values by using cheaper and smaller cations (K, Pb) instead of large cations in the NZP structure cavities.

The sulfate phosphate $Zr_2(PO_4)_2SO_4$ and the sulfates $R_2(SO_4)_3$ (R is a triply charged cation), $Li_xMg_xR_{2-x}(SO_4)_3$ (R = Al, Cr), $NaMgFe(SO_4)_3$, and $Na_{1+x}Mg_{1+x}In_{1-x}(SO_4)_3$ ($x = 0.2, 0.5$) crystallizing in the NZP type structure are known to date [17–20]. Using published data [20], we calculated the LTEC of $NaMgFe(SO_4)_3$ as $\alpha_{av} = 6.8 \times 10^{-6}{}^{\circ}C^{-1}$. This is a medium-expansion material. Low-expansion sulfate phosphates can be prepared by varying the composition without a change in the structure type.

The purpose of this study is the preparation of $NaFeZr(PO_4)_2SO_4$ and $Pb_{2/3}FeZr(PO_4)_{7/3}(SO_4)_{2/3}$

sulfate phosphates, more specific determination of their structure, and investigation of the thermal behavior and thermal expansion.

EXPERIMENTAL

$NaFeZr(PO_4)_2SO_4$ and $Pb_{2/3}FeZr(PO_4)_{7/3}(SO_4)_{2/3}$ were prepared by the sol–gel method followed by heat treatment. Reagent grade chemicals: NaCl, $Pb(NO_3)_2$, Fe_2O_3, $ZrOCl_2 \cdot 8H_2O$, H_3PO_4, and H_2SO_4 served as the starting compounds. Stoichiometric amounts of aqueous solutions of metal salts were poured together with continuous stirring at room temperature, and then solutions of sulfuric and phosphoric acids taken according to the sulfate phosphate stoichiometry were added. The reaction mixtures were dried at 90–130°C and heat treated in air at 600–750°C for at least 24 h in each stage. Each heating stage alternated with disintegration to provide homogenization of mixtures. For advancing the reaction, the powders were pressed into discs. In the case of $NaFeZr(PO_4)_2SO_4$, the highest temperature of the synthesis was 600°C, that for $Pb_{2/3}FeZr(PO_4)_{7/3}(SO_4)_{2/3}$ was 750°C. In the preparation of lead-containing sample, 2 wt % ZnO was used as the sintering additive promoting a tighter contact between grains, increasing the solid-state reaction rate, and decreasing the synthesis temperature [21]. Zinc oxide was added to the sample annealed at 700°C. The samples were polycrystalline red-brown powders.

The sample chemical composition and homogeneity were verified using a JEOL JSM-7600F high-resolution scanning electron microscope with a field emission gun (Schottky cathode) equipped with an OXFORD X-Max 80 energy dispersive spectrometer (Premium) with a semiconductor silicon drift detector and nitrogen-free cooling at an accelerating voltage of 15 and 20 kV. The results of microprobe analysis of single-phase samples demonstrated the homogeneity of grain composition and agreement with the theoretical values to within the error of the method (not more than 2 at %).

The X-ray diffraction measurements were carried out on a Shimadzu XRD-6000 diffractometer (CuK_α-radiation, $\lambda = 1.54178$ Å, $2\theta = 10°–60°$) equipped with an Anton Paar TTK 450 temperature chamber. The X-ray patterns were indexed by the structure analogy method using the crystal data of compounds described in the literature. The unit cell parameters of the obtained compounds were refined by the least-squares method. The X-ray diffraction patterns of the $Pb_{2/3}FeZr(PO_4)_{7/3}(SO_4)_{2/3}$ sample for structural studies were measured in the 2θ range of 10°–110° with a scanning step of 0.02° and a 16 s exposure in each point. The X-ray diffraction pattern treatment and structure refinement were performed by the Rietveld method [22] using the RIETAN-97 software [23]. The peak profiles were approximated with the modified pseudo-Voigt function (Mod-TCH pV [24]). The atom coordinates of $PbFeZr(PO_4)_3$ were used as the basic model for sulfate phosphate crystal structure refinement [25].

The thermal expansion was studied on the same diffractometer using the temperature chamber with a discrete mode of temperature variation in the range from −120 to 200°C with a 40–50°C step. The $Pb_{2/3}FeZr(PO_4)_{7/3}(SO_4)_{2/3}$ sample was cooled by a controlled liquid nitrogen flow. The temperature was measured with a Pt100 resistance temperature detector. At each chosen temperature, the range of 2θ angles was 10°–50°; silicon was used as the external standard.

The simultaneous TG–DTA analysis of sodium iron zirconium and lead iron zirconium sulfate phosphate gels pretreated at 130 and 300°C, respectively, and of crystalline sulfate phosphates was carried out under argon on a Labsys TG-DTA/DSC thermal analyzer in the temperature range of 25–1200°C at heating and cooling rates of 10K/min.

The functional composition of samples was confirmed by IR spectroscopic measurements. The IR absorption spectra were recorded on a FSM-1201 Fourier Transform IR spectrometer in the 400–1400 cm^{-1} wavelength range.

RESULTS AND DISCUSSION

The $NaFeZr(PO_4)_2SO_4$ and $Pb_{2/3}FeZr(PO_4)_{7/3}(SO_4)_{2/3}$ sulfate phosphates with expected NZP structure were predicted relying on the crystal data. The NZP family (basic structure $NaZr_2(PO_4)_3$, space group $R\bar{3}c$, $a = 8.8045$ Å, $c = 22.7585$ Å [26]) comprises compounds and solid solutions described by the crystal chemical formula $(M1)_{0\to1}(M2)_{0\to3}\{[L_2(TO_4)_3]^{p-}\}_{3\infty}$, where $\{[L_2(TO_4)_3]^{p-}\}_{3\infty}$ is the structure framework (p is the framework charge), while $(M1)_{0\to1}$, $(M2)_{0\to3}$ are different types of extra-framework cationic sites with designation of position occupancy in each type [2]. The structure framework is formed by LO_6 octahedra and TO_4 tetrahedra, which share vertices; the M1 and M2 vacancies of various size are convenient for the arrangement of a broad range of cations counterbalancing the framework charge. The structure-forming octahedral cations L with predominantly covalent nature of metal–oxygen bond are usually in oxidation states from +5 to +3. In the case of predicted compounds, the framework is formed by the ZrO_6 and FeO_6 octahedra and PO_4 and SO_4 tetrahedra. The extra-framework cations have lower oxidation states and greater radii. In our case, these are Na^+ or Pb^{2+} cations.

The $Zr^{4+} + P^{5+} \rightarrow Fe^{3+} + S^{6+}$ isomorphic substitution in the basic $NaZr_2(PO_4)_3$ structure gives rise to $NaFeZr(PO_4)_2SO_4$. Its formation is faced with some difficulty owing to the thermal instability at tempera-

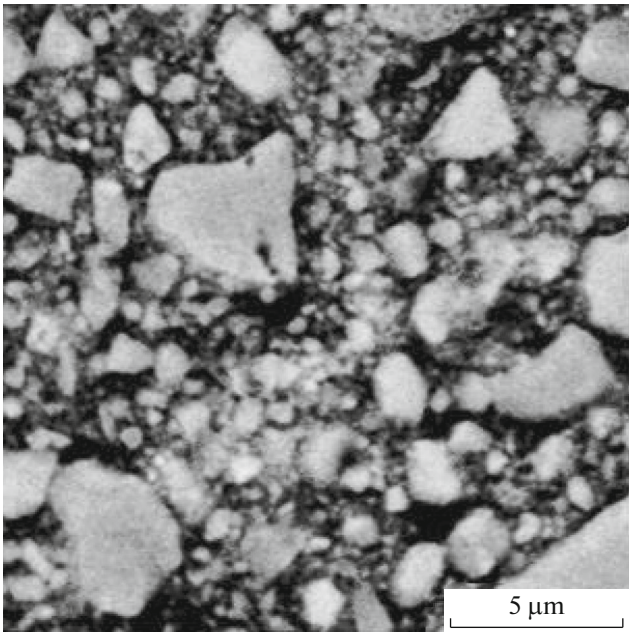

Fig. 1. Micrograph of the $NaFeZr(PO_4)_2SO_4$ sample.

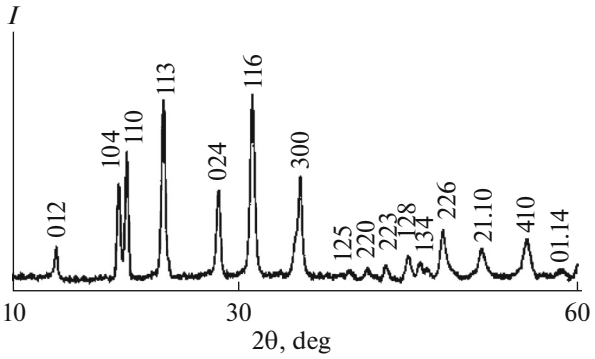

Fig. 2. X-ray diffraction pattern of the $NaFeZr(PO_4)_2SO_4$ sulfate phosphate.

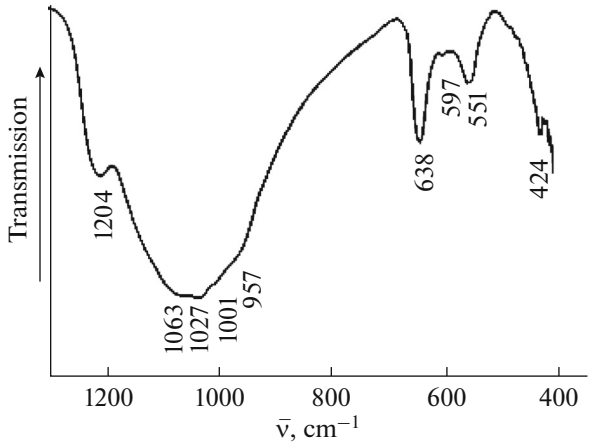

Fig. 3. IR spectrum of $Pb_{2/3}FeZr(PO_4)_{7/3}(SO_4)_{2/3}$.

tures above 600°C via partial loss of sulfur as SO_3. In the case of $Pb_{2/3}FeZr(PO_4)_{7/3}(SO_4)_{2/3}$, the specified stoichiometry of the final product makes it possible to bind the whole amount of sulfur in the initial reaction mixture to an intermediate refractory product—lead sulfate (with a melting point above 1000°C) and avoid the loss of sulfur during the synthesis.

The processes preceding the formation of the target $NaFeZr(PO_4)_2SO_4$ phase were studied by simultaneous thermal analysis (TG–DTA). In the temperature range from 100 to 600°C, the mass loss is accompanied by diffuse endothermic peaks in the DTA curve with minima at temperatures of 120 and 430°C; the major mass loss occurs below 200°C. The investigated temperature range corresponds to decomposition of zirconium hydrogen phosphate, which is formed during the reaction, evaporation of hydrogen chloride and water, and formation of the final product – mixed sodium iron zirconium sulfate phosphate according to the equation:

$$NaCl + 0.5Fe_2O_3 + ZrOCl_2 + 2H_3PO_4 + H_2SO_4 = NaFeZr(PO_4)_2SO_4 + 3HCl + 2.5H_2O.$$

The single-phase $NaFeZr(PO_4)_2SO_4$ was prepared upon grinding–pressing–annealing (600°C) cycle repeated many times. The obtained image of the sample leads to the conclusion that its grain structure is inhomogeneous, the grain size varying from 1 to 5 μm (Fig. 1). The microprobe analysis data demonstrated the homogeneity of grain composition being given by $Na_{0.98(3)}Fe_{1.02(5)}Zr_{0.99(3)}P_{2.06(4)}S_{0.95(4)}O_{12}$.

According to powder X-ray diffraction data, $NaFeZr(PO_4)_2SO_4$ (Fig. 2) crystallizes in the NZP structure (space group $R\bar{3}c$, $Z = 6$) with the following unit cell parameters: $a = 8.750(4)$ Å, $c = 22.626(9)$ Å, $V = 1500(1)$ Å^3. The powder X-ray diffraction data indicate that as the $NaFeZr(PO_4)_2SO_4$ is heated above 600°C, the unit cell parameters of the sample grow. This is related to a decrease in the content of SO_4 anions (which are smaller than PO_4) because of the partial loss of sulfur as SO_3. The thermal decomposition of $NaFeZr(PO_4)_2SO_4$ was studied by subjecting the sample to isothermal annealing at 650 and 700°C. The sample was kept at each temperature for 24 h. After the single-phase sample was kept at 650°C, the loss of sulfur was 60 wt % according to microprobe analysis data; after being kept at 700°C, the sample contained less than 20 wt % of the initial amount of sulfur and represented a mixture of $Na_{1.4}Fe_{0.6}Zr_{1.4}(PO_4)_{2.8}(SO_4)_{0.2}$ and Fe_2O_3 phases. The DTA curve of $NaFeZr(PO_4)_2SO_4$ showed an endotherm at 730°C associated with thermal decomposition.

As noted above, the sample stoichiometry can help to prevent the loss of sulfur during the synthesis of $Pb_{2/3}FeZr(PO_4)_{7/3}(SO_4)_{2/3}$. The powder X-ray diffrac-

Table 1. Data collection details and structure refinement parameters for $Pb_{2/3}FeZr(PO_4)_{7/3}(SO_4)_{2/3}$

Characteristics	$Pb_{2/3}FeZr(PO_4)_{7/3}(SO_4)_{2/3}$
Space group, Z	$R\bar{3}c$, 6
a, Å	8.6339(4)
c, Å	23.2991(9)
V, Å^3	1504.1(1)
$\rho_{X\text{-ray}}$, g/cm^3	4.159(1)
2θ range, deg	10.00–110.00
Scanning step	0.02
Number of reflections	214
Number of refined parameters	28
Reliability factors	
R_{wp}, %	3.24
R_p, %	2.20
S	2.9103

tion data indicate that a target phase with iron(III) oxide impurity is formed at 600°C. The degree of crystallinity increases with temperature rise and at 750°C, a single-phase sulfate phosphate with the NZP structure is formed.

The DTA of the reaction mixture with the stoichiometry $Pb_{2/3}FeZrP_{7/3}S_{2/3}O_{12}$ in combination with powder X-ray diffraction data indicate that the endotherms are related to decomposition of the starting reagents, which form the heterogeneous system (380°C), and to the crystallization (750°C) and its following decomposition, leading to formation of $PbFeZr(PO_4)_3$ (1195°C) with NZP structure as the major product.

The IR spectrum of $Pb_{2/3}FeZr(PO_4)_{7/3}(SO_4)_{2/3}$, space group $R\bar{3}c$, is presented in Fig. 3. In the $R\bar{3}c$ space group (D_{3d} point group), the PO_4^{3-} and SO_4^{3-} ions occupy positions on a 2 axis (C_2 site symmetry). The vibrations of C_2 site-symmetric ions are transformed in the following way: the A (ν_1) mode becomes active and the degeneracy of the $E \rightarrow 2A$ (ν_2) and $F_2 \rightarrow A + 2B$ (ν_3, ν_4) modes is completely eliminated. The D_{3d} point group leads to further transformation of the vibrations: $A \rightarrow E_u$ (ν_1), $2A \rightarrow 2E_u$ (ν_2), and $A + 2B \rightarrow 2A_{2u} + 3E_u$($\nu_3$, ν_4). Thus, in the IR spectrum, the selection rules allow five asymmetric stretching modes (ν_3), one symmetric stretching mode (ν_1), five asymmetric bending modes (ν_4), and two symmetric bending modes (ν_2) for each tetrahedral ion. Since the differences between the sulfur and phosphorus oxidation states and atomic masses are slight and the interatomic distances characteristic of the S–O and P–O bonds are similar for the same coordination number, the S–O and P–O vibration frequencies and the positions of bands in the spectrum of the sulfate phosphate coincide. The absorption bands at 1220–1000 cm^{-1} were assigned to ν_3 asymmetric stretching modes of the $(P,S)O_4$ ion. The appearance of the high-frequency band at 1204 cm^{-1} is attributable to a contribution of the electron density of the highly charged small Fe^{3+} and Zr^{4+} ions to the (P,S)–O bond. The band at ~957 cm^{-1} was assigned to the ν_1 symmetric stretching modes. The bands at 640–550 cm^{-1} are due to the ν_4 bending modes and the 424 cm^{-1} corresponds to the ν_2 bending mode of the tetrahedral (phosphate and sulfate) ions.

The structure of $Pb_{2/3}FeZr(PO_4)_{7/3}(SO_4)_{2/3}$ was refined for room temperature by the Rietveld method. Figure 4 shows the experimental and calculated line and difference X-ray diffraction patterns. The structure refinement proceeded from the data for the $PbFeZr(PO_4)_3$ analog (space group $R\bar{3}c$) [25]. The data collection details, unit cell parameters, and selected structure refinement details are given in Table 1.

The structure of $Pb_{2/3}FeZr(PO_4)_{7/3}(SO_4)_{2/3}$ corresponds to the NZP type. The refinement was carried out assuming that owing to similarity of the ionic radii and electronegativities, the Fe^{3+} and Zr^{4+} cations randomly occupy two crystallographically equivalent framework sites L octahedrally coordinated by oxygen atoms in the sulfate phosphate structure ($2 \times 12c$). The phosphorus and sulfur atoms occupy the only type of

Table 2. Atom coordinates and displacement parameters and occupancies (q) of the basis atoms in $Pb_{2/3}FeZr(PO_4)_{7/3}(SO_4)_{2/3}$

Atom	Site	x	y	z	B_{iso}	q
Pb	6b	0	0	0	1.94(7)	0.6667
Fe	12c	0	0	0.14933(9)	1.94(7)	0.5
Zr	12c	0	0	0.14933(9)	1.94(7)	0.5
S	18e	0.2834(6)	0	0.25	1.94(7)	0.2222
P	18e	0.2834(6)	0	0.25	1.94(7)	0.7778
O(1)	36f	0.1718(8)	–0.050(1)	0.1892(3)	1.94(7)	1.0
O(2)	36f	0.1957(7)	0.1653(7)	0.0969(3)	1.94(7)	1.0

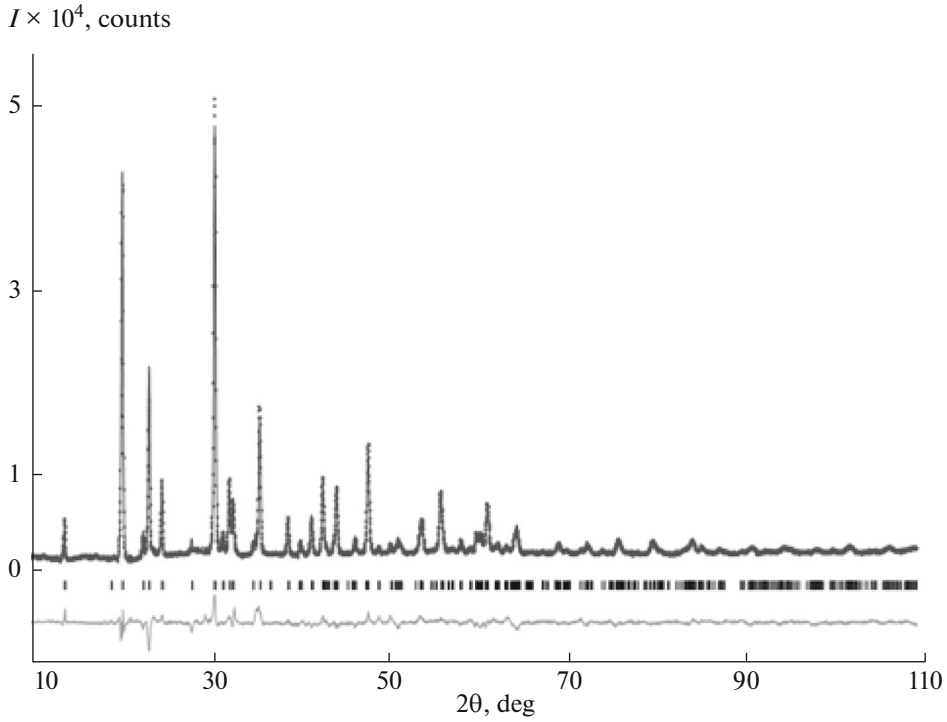

Fig. 4. Experimental (continuous line) X-ray diffraction spectrum of the synthesized sample and calculated (asterisks) X-ray diffraction spectrum of $Pb_{2/3}FeZr(PO_4)_{7/3}(SO_4)_{2/3}$. The vertical bars show the positions of reflections of the theoretical X-ray diffraction pattern, the curve in the lower part of the figure is the intensity difference curve between the experimental and theoretical spectra.

tetrahedrally coordinated framework cationic sites (18*e*). Relatively large Pb^{2+} ions occur in the M1 structure cavities, to occupy 2/3 of these sites. The refinement of Pb^{2+} occupation of extra-framework M2 cavities demonstrated that these sites remain vacant. The atom coordinates, displacement parameters, and basis atom occupancies are summarized in Table 2. The calculated bond lengths (Table 3) and bond angles are within the standard ranges for NZP phosphates and sulfates. A fragment of the $Pb_{2/3}FeZr(PO_4)_{7/3}(SO_4)_{2/3}$ structure is shown in Fig. 5.

The structure of $Pb_{2/3}FeZr(PO_4)_{7/3}(SO_4)_{2/3}$ comprises a framework of vertex-sharing $(Fe,Zr)O_6$ octahedra and $(P,S)O_4$ tetrahedra. The key structural unit of the framework is a lantern consisting of two octahedra and three tetrahedra. These lanterns form parallel columns arranged along the crystallographic *c* axis. The occupation of the tetrahedral sites in $Pb_{2/3}FeZr(PO_4)_{7/3}(SO_4)_{2/3}$ by sulfur cations, which are smaller than phosphorus, results in cell contraction along the crystallographic axes and distortion of tetrahedra. The (P,S)–O distance varies from 1.554 to 1.691 Å. The difference between the (P,S)–O bond lengths results in lantern twisting along the *a* axis and compression along the *c* axis (with respect to the lantern formed in the unsubstituted phosphate).

The possibility of using of mixed NZP sulfate phosphate for elucidating the relationship between the composition (determining the size of the rhombohedral cell) and the crystal thermal expansion parameters (controlled by the LTEC). The thermal expansion of the $Pb_{2/3}FeZr(PO_4)_{7/3}(SO_4)_{2/3}$ sulfate phosphate was studied by variable-temperature X-ray diffraction. The plots of unit cell parameters *a* and *c* vs. temperature are shown in Fig. 6. These plots are linear: both unit cell parameters increase with temperature, which is caused by the correlated rotation of the tetrahedra and octahedra around the *c* axis inherent in NZP compounds [9]. The thermal expansion coefficients of $Pb_{2/3}FeZr(PO_4)_{7/3}(SO_4)_{2/3}$ are: $\alpha_a = 0.97 \times 10^{-6}$, $\alpha_c = 3.2 \times 10^{-6}$, and $\alpha_{av} = 1.7 \times 10^{-6\circ}C^{-1}$. This compound refers to the low-expansion class. Both thermal expansion coefficients α_a and α_c are positive, $\alpha_a < \alpha_c$, which brings about some anisotropy. The thermal expansion

Table 3. Selected interatomic distances in the $(Fe,Zr)O_6$ and $(P,S)O_4$ polyhedra in $Pb_{2/3}FeZr(PO_4)_{7/3}(SO_4)_{2/3}$

Bond	*d*, Å	Bond	*d*, Å
Pb–O2 (×6)	2.744(7)	(P,S)–O1 (×2)	1.691(8)
(Fe,Zr)–O1 (×3)	1.775(5)	(P,S)–O2 (×2)	1.554(5)
(Fe,Zr)–O2 (×3)	2.016(6)		

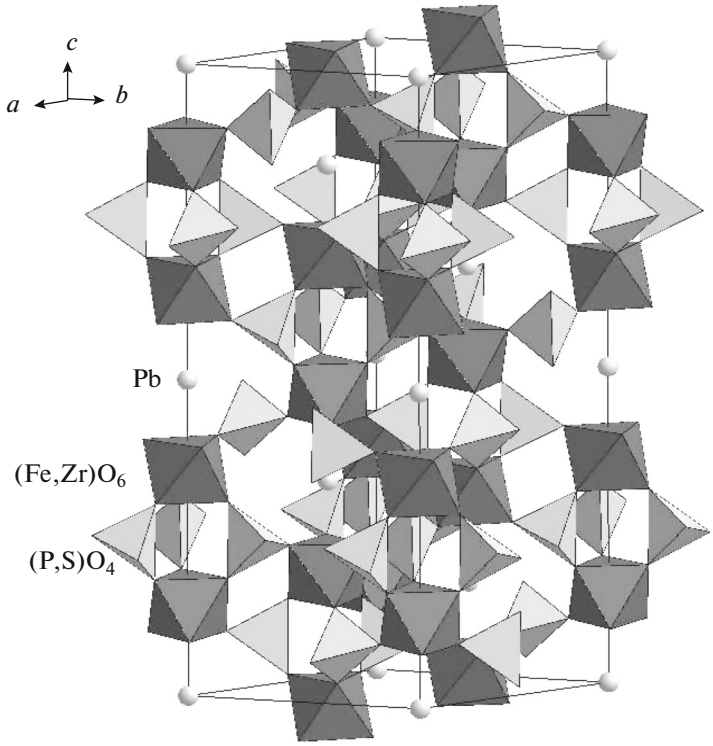

Fig. 5. Fragment of the structure of $Pb_{2/3}FeZr(PO_4)_{7/3}(SO_4)_{2/3}$.

anisotropy is $|\alpha_a - \alpha_c|$ is 2.2 $\times 10^{-6}K^{-1}$. As we suggested, targeted combination of different tetrahedral anions, of which one is phosphorus and the other (smaller) one is sulfur, in an NZP structure resulted in a decrease in the framework dimensions and cavities. Thus, we were able to obtain low-expansion sulfate phosphate with smaller extra-framework cation (cheap Pb) instead of larger (and more expensive) cations commonly used in monoanionic phosphates.

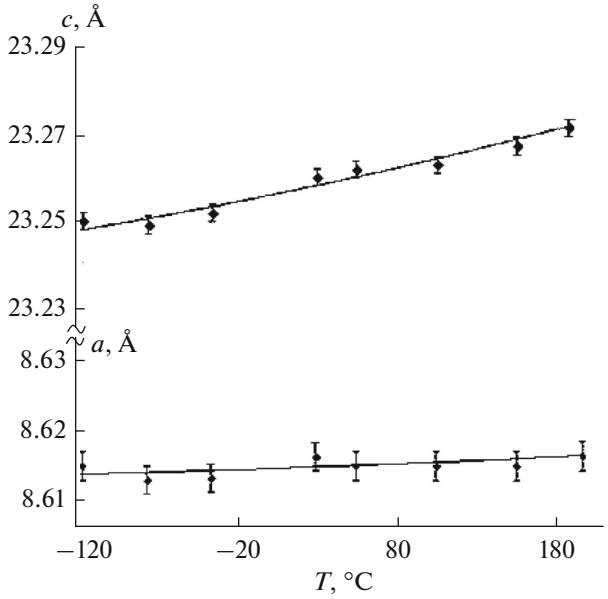

Fig. 6. Unit cell parameters of $Pb_{2/3}FeZr(PO_4)_{7/3}(SO_4)_{2/3}$ vs. temperature.

Thus, the deliberate search for compounds with the NZP structure and low thermal expansion resulted in the synthesis of mixed sulfate phosphates, $NaFeZr(PO_4)_2SO_4$ and $Pb_{2/3}FeZr(PO_4)_{7/3}(SO_4)_{2/3}$. The phase formation, thermal stability, and thermal expansion of the products were studied. The $Pb_{2/3}FeZr(PO_4)_{7/3}(SO_4)_{2/3}$ sulfate phosphate has low volume thermal expansion with slight anisotropy. The results of our study exten the published data on mixed NZP phosphates. By varying the composition of the sulfate phosphates while retaining the stable structural units (lanterns) forming the crystal frame, one can smoothly adjust the unit cell size (and symmetry) and finely correct the thermal expansion parameters using abundant and available elements.

ACKNOWLEDGMENTS

This work was supported by the Russian Foundation for Basic Research within the framework of project no. 15-03-00716_a.

REFERENCES

1. M. E. Brownfield, E. E. Foord, S. J. Sutley, et al., Am. Mineral. **78**, 653 (1993).
2. V. I. Pet'kov, Russ. Chem. Rev. **81**, 606 (2012).
3. M. V. Sukhanov, V. I. Pet'kov, V. S. Kurazhkovskaya, et al., Russ. J. Inorg. Chem. **51**, 706 (2006).
4. M. V. Sukhanov, V. I. Pet'kov, D. V. Firsov, et al., Russ. J. Inorg. Chem. **56**, 1351 (2011).
5. V. I. Pet'kov, M. V. Sukhanov, A. S. Shipilov, et al., Russ. J. Inorg. Chem. **58**, 1015 (2013).
6. V. I. Pet'kov, M. V. Sukhanov, A. S. Shipilov, et al., Inorg. Mater. **50**, 263 (2014).
7. V. I. Pet'kov, A. S. Shipilov, M. V. Sukhanov, et al., Russ. J. Inorg. Chem. **59**, 1201 (2014).
8. A. K. Ivanov-Shits and I. V. Murin, *Solid-State Ionics* (Izd. SPbGU, St. Petersburg, 2001), Vol. 1 [in Russian].
9. V. I. Pet'kov and A. I. Orlova, Inorg. Mater. **39**, 1013 (2003).
10. N. Anantharamulu, Rao K. Koteswara, G. Rambabu, et al., J. Mater. Sci. **46**, 2821 (2011).
11. V. I. Pet'kov, A. I. Orlova, G. N. Kasantsev, et al., J. Therm. Anal. Cal. **66**, 623 (2001).
12. S. Y. Limaye, D. K. Agrawal, and H. A. McKinstry, J. Am. Ceram. Soc. **70**, 232 (1987).
13. H. Miyazaki, I. Ushiroda, D. Itomura, et al., Jpn. J. Appl. Phys. **47**, 7262 (2008).
14. B. Zhang and J. Guo, J. Eur. Ceram. Soc. **15**, 929 (1995).
15. P. Oikonomou, Ch. Dedeloudis, C. J. Stournaras, et al., J. Eur. Ceram. Soc. **27**, 1253 (2007).
16. V. I. Pet'kov and E. A. Asabina, Glass Ceram., **61**, 233 (2004).
17. J. Alamo and R. Roy, J. Solid State Chem. **51**, 270 (1984).
18. R. Masse, J. C. Guitel, and R. Perret, Bul. Soc. Fr. Mineral. Crist. **96**, 346 (1973).
19. P. R. Slater and C. Greaves, J. Mater. Chem. **2**, 1267 (1992).
20. P. R. Slater and C. Greaves, J. Mater. Chem. **4**, 1469 (1994).
21. M. V. Sukhanov, V. I. Pet'kov, and D. V. Firsov, Inorg. Mater. **47**, 674 (2011).
22. H. M. Rietveld, Acta Crystallogr. **22**, 151 (1967).
23. Y. I. Kim and F. Izumi, J. Ceram. Soc. Jpn. **102**, 401 (1994).
24. F. Izumi, *The Rietveld Method*, Ed. by R. A. Ch. Young (Oxford Univ. Press, New York, 1993).
25. G. Buvanesvari and U. V. Varadaraju, J. Solid State Chem. **145**, 227 (1999).
26. H. Y-P. Hong, Mater. Res. Bul. **11**, 173 (1976).

Translated by Z. Svitanko